IMPROVING THE MATHEMATICAL MODEL FOR LUMINESCENT DOWN-SHIFTING LAYERS BY INVESTIGATING THEIR LOSS MECHANISMS

M. Rafiee*, H. Ahmed, S. Chandra and S. J. McCormack
Dept. of Civil, Structural and Environmental Engineering, Trinity College Dublin, Dublin 2, Ireland
* Corresponding author. Email: rafieem@tcd.ie Tel: +353 1 896 2671

ABSTRACT: A Luminescent Down-Shifting (LDS) layer is an optical approach to improve the solar cell's optical response by using luminescent species doped in a polymer matrix material to form a thin layer to be deposited on top of the PV solar cell. In this article, the performance of different polymer matrix materials with various loss mechanisms (attenuation and scattering losses) are mathematically modeled based on a ray tracing algorithm. The simulation is carried out with and without counting the loss mechanisms in the mathematical model. First, the model studied the performance of LDS layer ($12.49 \times 12.49 \times 0.015$ cm) of Europium complex (Eu) doped in a Polyvinyl Acetate (PVA) film and deposited on top of monocrystalline Silicon (c-Si) under standard AM1.5 global solar radiation. The comparison of the modelling and experimental results proved that the model's discrepancy was improved from 27% to 2% when the loss mechanisms of the matrix materials are counted in the model. Optical efficiency of 80% was obtained for the LDS layer and an excellent agreement has been achieved between the experimental and model results. Subsequently, the model was used to study the performance of other matrix materials such as glass, epoxy resin polymer, and Poly Methyl Methacrylate (PMMA) polymer for their loss mechanisms. The results have shown that although these polymer are transparent above 300 nm, their optical response significantly changes in the region between 300 to 400 nm hence the optical efficiency and response of the LDS layer.

Keywords: Luminescent Down Shifting, Ray Tracing, Matrix Material, Loss Mechanisms, Optical Efficiency, Emission, Absorption

1 INTRODUCTION

In all Photovoltaic (PV) technologies developed to date, the poor optical response for short wavelength light represents a fundamental limit to the maximum efficiency achieved by the solar cell. In this region (300-500 nm), the high energy photons are not used efficiently and their energy is lost through thermalisation (Rothemund, 2014). The potential exists to increase solar cell efficiency by making better use of short wavelength solar radiation. As is seen in Fig. 1, LDS layer is an optical approach to improve the solar cell's optical response by using luminescent species doped in a polymer matrix material to form a thin layer to be deposited on top of the PV solar cell (Ahmed, 2014, Hovel et al., 1979).
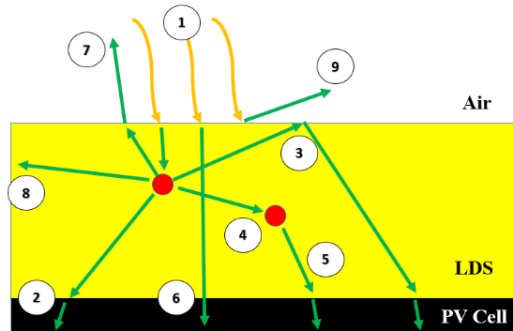
Figure 1: Configuration of LDS which shows: 1- photon enters the LDS absorbed by the luminescent material. Then, 2- re-emitted at longer wavelength and reaches the PV cell 3- or it is wave-guided to the PV cell by Total Internal Reflection (TIR) 4- or re-absorbed by another luminescent molecule and 5- re-emitted with less energy and then reaches the PV cell. 6- Some photons directly reach the PV cell without red-shifting. The other losses include: 7- escape cone loss 8- edge losses and 9- front surface reflection. Note that, the light may also be scattered or attenuated by the matrix material which is not shown here

LDS layers can convert both diffuse and direct solar radiation; therefore, it is an adequate technology where diffuse solar radiation is dominant, such as in northern European countries where over 50% of light is diffuse (van Sark et al., 2008). These features make them a preferred choice for use in Building Integration Photovoltaic (BIPV) systems and façades of buildings which brings us closer to the goal of constructing buildings with zero carbon energy consumption and buildings which are able to cover their required energy by renewable energies (Aste et al., 2011, Pagliaro et al., 2010, Debije and Verbunt, 2012).

In LDS layers, the luminescent species absorbs the short wavelength solar radiation and emits at longer wavelengths where the external quantum efficiency (EQE) of the solar cell is higher. EQE is defined as the ratio of the number of collected electrons to the number of incident photons (Wenham, 2012, Solanki, 2015, Radziemska, 2006, Wen et al., 2012, Abderrezek et al., 2013, Şahin and Ilan, 2013):

$$EQE(\lambda) = \frac{me(\lambda)}{mp(\lambda)} = IQE(\lambda) \times (1 - R_{PV}) \qquad (1)$$

Where $me(\lambda)$ is the number of electrons generated by the PV, $mp(\lambda)$ is the number of photons striking the PV at each wavelength, IQE is the internal quantum efficiency which is the ratio of the collected electrons to the absorbed photons by the PV and R_{PV} is the probability of the reflectance by the PV (Yang et al., 2008). When solar radiation is incident on the PV solar cell, the absorption probability is rapidly reduced due to two main loss sources: optical and recombination losses (Rothemund, 2014). This significantly decreases the External Quantum Efficiency (EQE) of the solar cell (Wilson and Richards, 2009).

It is cost effective to use modeling methods to design and optimize the LDS configuration before fabricating

actual LDS/PV. Thermodynamic or Ray Tracing methods (Kerrouche et al., 2014, Batchelder et al., 1979, Burgers et al., 2005, Parel et al., 2015, Barnham et al., 2000, Hughes et al., 2015, Glassner, 1989, Kennedy et al., 2007, Chatten et al., 2004, Earp et al., 2004, Carrascosa et al., 1983) can be used to model LDS while the accuracy of both models were similar (Farrell et al., 2005). Ray tracing algorithms are more time consuming in comparison with thermodynamic models (Glassner, 1989). However, the ray trace model is more flexible and can simulate different geometries and shapes with multiple luminescent species under diffuse and direct light (van Sark et al., 2008).

In this paper, LDS layer with EU^{3+} complex doped in PVA matrix was modelled using a ray tracing algorithm with and without counting the PVA matrix loss mechanisms (attenuation and scattering losses). The modeling and experimental results (Liu et al., 2013) were compared to validate the ray tracing algorithm. Subsequently, the model was run for LDS layers with different matrix materials such as glass, epoxy resin, and PMMA of the same size and configuration. The results were compared to investigate the loss mechanisms effect on the LDS layer efficiency and optical response.

2 MATHEMATICAL LDS MODELLING USING A RAY TRACING ALGORITHM

The LDS ray tracing algorithm is based on a set of ray intersection routines due to phenomena such as reflection, refraction, absorbing, scattering, attenuating and TIR events occurs inside the device. Each ray of light with specific wavelength and direction is traced until it leaves the system (Glassner, 1989). The routines are applied in an iterative loop for each ray irradiated to the device based on the exposed light spectrum. When a ray strikes the top surface of the LDS layer, it is either reflected or refracted according to the light incident angle as Snell's Law (Glassner, 1989). After refraction, the ray may be scattered or/and attenuated by the matrix material, lost as escape cone loss, absorbed and then emitted by the luminescent materials or wave-guided by TIR. The routine is continued until the fate of the ray is determined and then the same process is executed for the other rays. The occurrence probability of each event at each stage of the ray tracing algorithm is determined according to parameters such as wavelength, angle of the illuminated ray, characteristics of the matrix/ luminescent material, dimensions and configuration of the LDS layer. After implementing the iterative loop for all input rays, the optical efficiency of the device is calculated by:

$$\eta_{opt} = \frac{\int_{\lambda_{min}}^{\lambda_{max}} E_{P_{OUT}}(\lambda).d(\lambda)}{\int_{\lambda_{min}}^{\lambda_{max}} E_{P_{IN}}(\lambda).d(\lambda)} \qquad (2)$$

Where $E_{P_{OUT}}(\lambda)$ is the energy spectrum of the output photons detected by the PV and $E_{P_{IN}}(\lambda)$ is energy spectrum of the input solar radiation.

To evaluate the performance of the LDS/PV device, the EQE of the PV with and without the LDS layer is modelled by (Rothemund, 2014):

$$EQE_{LDS}(\lambda) = (\eta_{opt}.ESM.f_{abs}(\lambda)) + (EQE_{PV}(\lambda).f_{trans}(\lambda)) \qquad (3)$$

Where EQE_{PV} is the EQE of the solar cell without the LDS. $f_{abs} = 1 - e^{-\alpha d}$ is the absorption function of the luminescent material which gives the number of photons absorbed (α is the absorption coefficient in 1/mm and d is thickness of the LDS in mm). $f_{trans} = 1 - f_{abs}$ is the transmission function of the luminescent material which gives the number of photons transmitted through the layer. ESM (Emission Spectral Matching) is a factor that is used to normalize emission spectra and also match it to the EQE_{PV}:

$$ESM = \frac{\int_{\lambda_{min}}^{\lambda_{max}} PL(\lambda).EQE_{PV}(\lambda).d(\lambda)}{\int_{\lambda_{min}}^{\lambda_{max}} PL(\lambda).d(\lambda)} \qquad (4)$$

Where PL is the photoluminescence (or emission spectrum) of the luminescent material.

3 RESULTS, VALIDATION AND DISCUSSION

In this section, the experimental results of LDS doped with EU^{3+} complex (Liu et al., 2013) are used to validate the mathematical ray tracing modelling. The absorption and emission spectra of the luminescent material is shown in Fig. 2. The size of the LDS layer is 156 cm^2 with 0.15 mm thickness, deposited on top of c-Si PV. The radiation used in the experiment and modelling was AM 1.5 global solar radiation whose information obtained from ASTM G173-03 Reference Spectra. The concentration of the EU^{3+}complex was 1%.
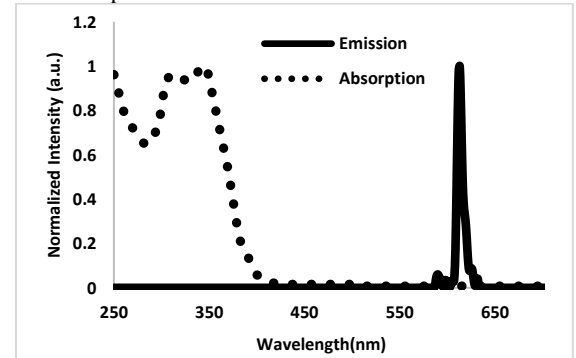
**Figure 2**: Normalized emission and absorption spectra for EU^{3+} complex (Liu et al., 2013)

The LDS based PVA layer was simulated under 250,000 rays while all loss mechanisms were considered in the modelling. Fig. 3.a shows the simulation and experimental output spectrum of the LDS (in arbitrary units) which are compared with the input solar radiation of the LDS layer. As it can be seen, the output spectrum of the LDS layer has a peak at around 610 nm which is due to the emission peak of the EU^{3+} complex. The input irradiation is red-shifted 60 nm (from 300 nm to 360nm) by the LDS layer. Fig.3.b shows the simulation and the experimental EQE_{LDS} curves in comparison with the EQE of uncoated PV. As can be seen, the EQE of the PV is significantly improved by around 46% in the wavelength range of 300-365nm due to the presence of the LDS layer. The achieved outputs of the model can be seen in Table I. In the PVA modelling, around 17% of rays is reflected after striking the top surface of the LDS layer due to the mismatching in refraction index of air (1) and the PVA film (1.49). It has been found that, 2.7% of rays were lost

as heat which is due to either attenuation/scattering loss of the PVA matrix material or non-unity quantum yield of the luminescent material. Majority of rays (~80%) reached the PV cell at the bottom layer which resulted in approximately 79% optical efficiency and a 31.39 $mA.cm^{-2}$ current density. It is observed that by counting the loss mechanisms, the model is valid and the simulation results are in an excellent agreement with experiments (maximum 2.2% discrepancy error in peak).

In the next step, the LDS based PVA layer was simulated (250,000 rays) but without counting the loss mechanisms of the PVA matrix material. As it can be seen in Fig.4, the modelling and experimental spectra are not well-matched in this case. In addition, as is seen in Table. 1, in the case where the loss mechanisms were not counted, the number of rays lost as heat decreased from 2.69% (in PVA modelling) to 1.01% (Without loss modelling) and that is due to the non-unity quantum yield of the luminescent material. This results in the final optical efficiency of 81% and gives a current density of 31.41 $mA.cm^{-2}$ without considering the losses in the model. As is seen, by considering loss mechanisms, the discrepancy error in the peak is enhanced from around 27% (Without loss modelling) to 2% (PVA modelling). This clearly shows the effect of counting material losses in the LDS modeling.

(a)

(b)
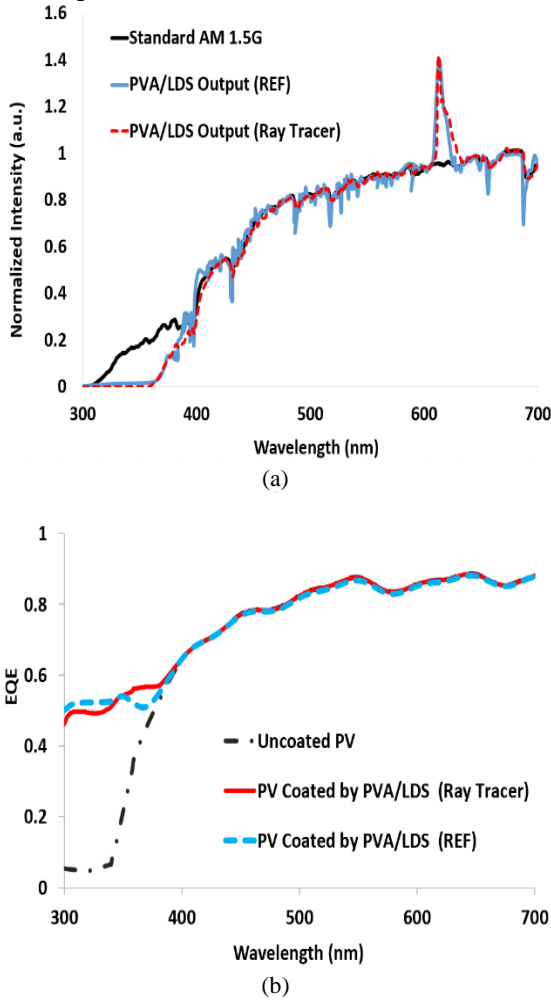
Figure 3: (a) Output spectrum of the LDS based PVA layer obtained from modeling (red) and experimental (blue) in comparison with the input solar radiation spectrum (black) and (b) Modeling (red) and experimental

(blue) EQE_{LDS} curves in comparison with the EQE of uncoated c-Si PV cell (black).
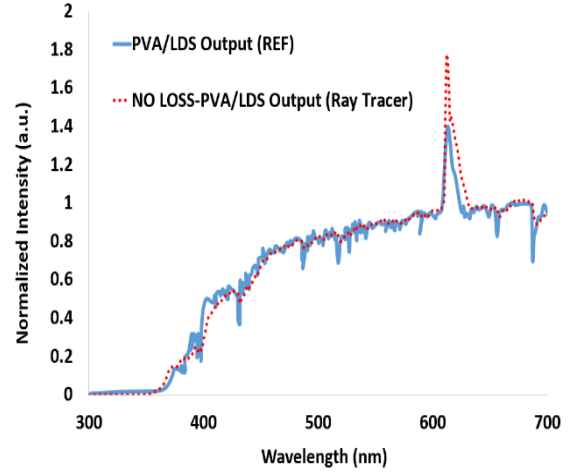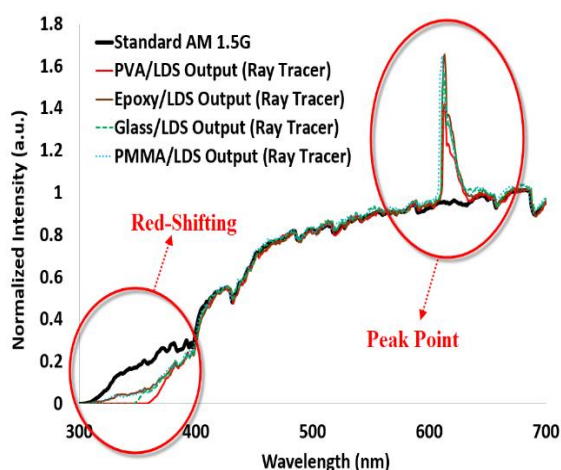

Figure 4: Output spectrum of the LDS based PVA layer obtained from modeling (red and no loss mechanisms is counted) and experimental (blue)

Table I: Statistic results obtained by the ray tracing model for LDS devices modelled with different matrix materials

Modelled Matrix Material	PVA	Without Loss	Glass	Epoxy Resin	PMMA
Number of Input Rays	250,000				
Reflected (%)	17.03	16.86	17.05	16.99	16.92
Refracted (%)	82.97	83.14	82.95	83.01	83.08
Lost as Heat (%)	2.69	1.01	2.44	0.87	1.02
Escape Cone Loss (%)	0.01	0.01	0.003	0.01	0.01
Reached to PV (%)	80.27	82.12	80.50	82.13	82.05
Optical Efficiency (%)	79.45	81.31	79.85	81.52	81.43
J_{sc} $(mA.cm^{-2})$	For Uncoated PV : 31.19 $mA.cm^{-2}$				
	31.39	31.41	31.39	31.41	31.40
Red-Shifting (nm)	In REF: 63nm				
	60	53	48	15	18
Discrepancy Error in Peak Point in comparison with the REF PVA Layer(%)	2.2	27.34	13.77	19.57	18.84

In the next step, LDS based Epoxy, Glass and PMMA were simulated under same conditions for the LDS layer (250,000 rays). As can be seen in Table 1, by using resin epoxy as the matrix material of the LDS, the least rate of lost as heat (0.87%) was achieved in comparison with other host materials. This resulted in the highest amount of optical efficiency (81.52%) and current density (31.41 $mA.cm^{-2}$). The resulted output spectra of the modelled devices are shown in Fig.5. As can be seen, the trend and the position of the peaks in all layers are similar; however, the red-shifting and the discrepancy error in the peak are different. This is due to the different absorption spectra of the matrix materials resulting in different loss mechanisms over wavelength which can significantly change the optical response of the LDS layer.

Figure 5: Output spectrums of LDS layers based, epoxy, glass and PMMA compared to the solar radiation spectrum. The LDS PVA layer emission is also shown.

4   CONCLUSION

In this paper, different matrix polymer materials with various loss mechanisms were modeled in LDS layer encapsulation by using a ray tracing algorithm. First, the developed model simulated the performance of an LDS layer of EU^{3+} doped in PVA film on top of c-Si PV cell. It was found that, when loss mechanisms (attenuation and scattering) are counted in the model algorithm, the model's discrepancy in comparison with the experimental results, is significantly improved from around 27% to 2%. By considering the losses, an excellent agreement has been achieved between the experimental and the model results. By using the developed model, the LDS layer achieved 79% optical efficiency and 31.39 mA.cm^{-2} current density. In addition, the EQE of the PV is significantly improved by around 46% in the wavelength range of 300-365nm.

Second, the model was used to simulate the performances of LDS based glass, epoxy and PMMA layers to see the effect of the loss mechanisms for these matrix materials. The best results were achieved by LDS based epoxy layer with around 82% optical efficiency and 31.41 mA.cm^{-2} current density. Different amounts of red-shift was observed in the modelled LDS layers when compared to the solar radiation spectrum. Therefore, the selection of the matrix material is very important when designing the LDS layer. The matrix material must be a suitable environment for the luminescent species and should exhibit a high transmittance and low scattering over the LDS operating wavelength, 300-500 nm. Also, the matrix materials should be highly transparent in the region where the PV cell is efficient so that it does not attenuate the incident rays in this region. It has been observed that, all used matrix materials are transparent after ~ 300nm; however, their optical response in the region between 300-400nm can significantly change the response and optical properties of LDS layer.

5   ACKNOWLEDGEMENT

6   References

ABDERREZEK, M., FATHI, M., DJAHLI, F. & AYAD, M. 2013. Numerical Simulation of Luminescent Downshifting in Top Cell of Monolithic Tandem Solar Cells. *International Journal of Photoenergy,* 2013.

AHMED, H. 2014. *Materials Characterization And Plasmonic Interaction In Enhanced Luminescent Down-Shifting Layers For Photovoltaic Devices.* PhD, Dublin Institute of Technology.

ASTE, N., ADHIKARI, R. & DEL PERO, C. Photovoltaic technology for renewable electricity production: Towards net zero energy buildings. Clean Electrical Power (ICCEP), 2011 International Conference on, 2011. IEEE, 446-450.

BARNHAM, K., MARQUES, J. L., HASSARD, J. & O'BRIEN, P. 2000. Quantum-dot concentrator and thermodynamic model for the global redshift. *Applied Physics Letters,* 76**,** 1197-1199.

BATCHELDER, J., ZEWAI, A. & COLE, T. 1979. Luminescent solar concentrators. 1: Theory of operation and techniques for performance evaluation. *Applied Optics,* 18**,** 3090-3110.

BURGERS, A., SLOOFF, L., KINDERMAN, R. & VAN ROOSMALEN, J. Modelling of luminescent concentrators by ray-tracing. Presented at the 20th European Photovoltaic Solar Energy Conference and Exhibition, 2005. 10.

CARRASCOSA, M., UNAMUNO, S. & AGULLO-LOPEZ, F. 1983. Monte Carlo simulation of the performance of PMMA luminescent solar collectors. *Applied Optics,* 22**,** 3236-3241.

CHATTEN, A., BARNHAM, K., BUXTON, B., EKINS-DAUKES, N. & MALIK, M. 2004. Quantum dot solar concentrators. *Semiconductors,* 38**,** 909-917.

DEBIJE, M. G. & VERBUNT, P. P. 2012. Thirty years of luminescent solar concentrator research: solar energy for the built environment. *Advanced Energy Materials,* 2**,** 12-35.

EARP, A. A., SMITH, G. B., SWIFT, P. D. & FRANKLIN, J. 2004. Maximising the light output of a Luminescent Solar Concentrator. *Solar Energy,* 76**,** 655-667.

FARRELL, D., CHATTEN, A., JERMYN, C., THOMAS, P. & BARNHAM, K. Thermodynamic Modelling of the Luminescent Solar Concentrator. INTERNATIONAL SOLAR ENERGY SOCIETY UK SECTION-CONFERENCE-C, 2005. 179.

GLASSNER, A. S. 1989. *An introduction to ray tracing*, Elsevier.

HOVEL, H., HODGSON, R. & WOODALL, J. 1979. The effect of fluorescent wavelength shifting on solar cell spectral response. *Solar Energy Materials,* 2**,** 19-29.

HUGHES, M. D., WANG, S.-Y., BORCA-TASCIUC, D.-A. & KAMINSKI, D. A. 2015. Analysis of ultra-thin crystalline silicon solar cells coupled to a

luminescent solar concentrator. *Solar Energy,* 122**,** 667-677.

KENNEDY, M., ROWAN, B., MCCORMACK, S., DORAN, J. & NORTON, B. 2007. Ray-trace modelling of Quantum Dot Solar Concentrators and comparison with fabricated devices.

KERROUCHE, A., HARDY, D. A., ROSS, D. & RICHARDS, B. S. 2014. Luminescent solar concentrators: From experimental validation of 3D ray-tracing simulations to coloured stained-glass windows for BIPV. *Solar Energy Materials and Solar Cells,* 122**,** 99-106.

LIU, J., WANG, K., ZHENG, W., HUANG, W., LI, C. H. & YOU, X. Z. 2013. Improving spectral response of monocrystalline silicon photovoltaic modules using high efficient luminescent down-shifting Eu3+ complexes. *Progress in Photovoltaics: Research and Applications,* 21**,** 668-675.

PAGLIARO, M., CIRIMINNA, R. & PALMISANO, G. 2010. BIPV: merging the photovoltaic with the construction industry. *Progress in Photovoltaics: Research and Applications,* 18**,** 61-72.

PAREL, T. S., PISTOLAS, C., DANOS, L. & MARKVART, T. 2015. Modelling and experimental analysis of the angular distribution of the emitted light from the edge of luminescent solar concentrators. *Optical Materials,* 42**,** 532-537.

RADZIEMSKA, E. 2006. Effect of temperature on dark current characteristics of silicon solar cells and diodes. *International Journal of Energy Research,* 30**,** 127-134.

ROTHEMUND, R. 2014. Optical modelling of the external quantum efficiency of solar cells with luminescent down-shifting layers. *Solar Energy Materials and Solar Cells,* 120**,** 616-621.

ŞAHIN, D. & ILAN, B. 2013. Radiative transport theory for light propagation in luminescent media. *JOSA A,* 30**,** 813-820.

SOLANKI, C. S. 2015. *Solar photovoltaics: fundamentals, technologies and applications*, PHI Learning Pvt. Ltd.

VAN SARK, W. G., BARNHAM, K. W., SLOOFF, L. H., CHATTEN, A. J., BÜCHTEMANN, A., MEYER, A., MCCORMACK, S. J., KOOLE, R., FARRELL, D. J. & BOSE, R. 2008. Luminescent Solar Concentrators-A review of recent results. *Optics Express,* 16**,** 21773-21792.

WEN, C., FU, C., TANG, J., LIU, D., HU, S. & XING, Z. 2012. The influence of environment temperatures on single crystalline and polycrystalline silicon solar cell performance. *Science China Physics, Mechanics and Astronomy,* 55**,** 235-241.

WENHAM, S. R. 2012. *Applied photovoltaics*, Routledge.

WILSON, L. & RICHARDS, B. 2009. Measurement method for photoluminescent quantum yields of fluorescent organic dyes in polymethyl methacrylate for luminescent solar concentrators. *Applied optics,* 48**,** 212-220.

YANG, W., MA, Z., TANG, X., FENG, C., ZHAO, W. & SHI, P. 2008. Internal quantum efficiency for solar cells. *Solar Energy,* 82**,** 106-110.